

Effects of charging and tunnelling in a structure based on magic and non-magic metal clusters

V V Pogosov and E V Vasyutin

Department of Microelectronics and Semiconductor Devices, Zaporozhye National Technical University, Zhukovsky Street 63, Zaporozhye 69064, Ukraine

E-mail: vpogosov@zntu.edu.ua

Received 7 March 2006

Published 15 June 2006

Online at stacks.iop.org/Nano/17/3366

Abstract

The effects of charging and single-electron tunnelling in a metal cluster structure are investigated theoretically. In the framework of the particle-in-a-box model for spherical and disc-shaped gold clusters, the electron spectrum and the temperature dependence of the electron chemical potential are calculated. The difference between the electron chemical potentials of massive electrodes and islands leads to the noticeable charging of the electrode. We show that the effective residual charge is equal to the non-integer value of the elementary charge e and depends on the shape of the cluster. The equations for the analysis of the current–voltage characteristic are used under the conditions of conservation of the total energy of the structure, taking into account the contact potential difference. Restrictions associated with the Coulomb instability of a cluster are introduced into the theory in a simple way. It is shown that the critical charge of the cluster in an open electron system is close to the effective residual charge. For single-electron molecular transistors based on small gold clusters the current gap and its voltage asymmetry are computed. We demonstrate that the current gap exhibits non-monotonic size dependences which are related to the quantization of the electron spectrum and the Coulomb blockade.

(Some figures in this article are in colour only in the electronic version)

1. Introduction

Metal granules which are weakly coupled via tunnel barriers to electron reservoirs are of considerable interest in the physics of low-dimensional systems (see [1–4] and references therein).

The tunnelling current flowing through two massive electrodes can be controlled if a cluster is placed between them. At first sight, the probability of electron tunnelling (and consequently the value of the current) should be much greater in the presence of a granule between the reservoirs than in the case of its absence. However, the opposite behaviour (see the inset in figure 2(a) of [5]) was observed in experiments on spherical-like [5–7] and disc-shaped [8, 9] small clusters. The measured I – V characteristics have a plateau of zero current (a current gap).

In [5–7] a structure with two tunnel junctions (figure 1) was represented by a thick Au (111) film covered by a $d_c \sim$

10 Å thick dielectric layer (with dielectric constant $\epsilon \approx 3$), on which small spherical-like gold clusters were organized. The tungsten tip (with a slight curvature of the surface) of an STM microscope was covered by a gold film of thickness 10^3 Å. Therefore we can consider all three electrodes (two of them with a flat surface) as being gold.

Earlier, a similar STM (Pt/Ir tip) measurement for such a structure ($d_c \sim 14$ Å, $\epsilon \sim 2.7$) based on gold islands with monatomic height $H \approx 2.5$ Å (disc-shaped clusters) was carried out in [8, 9].

The experiments demonstrated the following features of the $I(V)$ behaviour:

- (1) The gap width of the zero conductance is *approximately* proportional to the *inverse radius* of the spheres (figures 1(c) and 2(a) in [5]) and discs (figure 4 in [8]). This does not allow one to establish unequivocally a

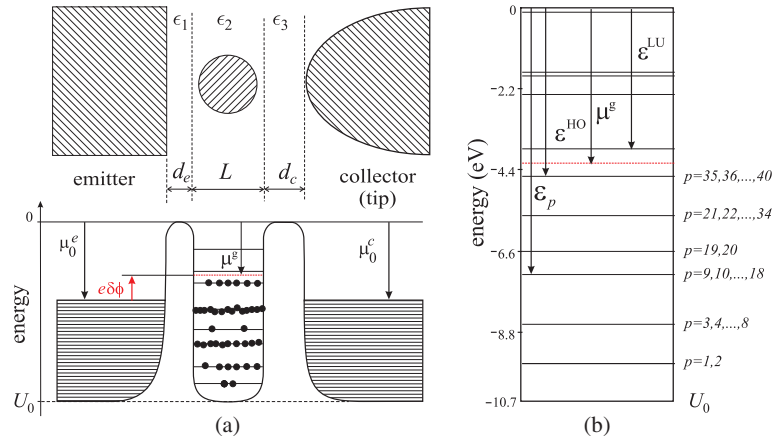


Figure 1. (a) The energy diagram at $T = 0$ for the structure Au/Au₄₀/Au before application of a voltage. In experiments [5–9] $\epsilon_1 = \epsilon_2 = \epsilon_3 = 1$. (b) The part of the energy spectrum for a spherical magic cluster Au₄₀.

classical or quantum origin for the gap. On the other hand, out of the current gap, the steps of the staircase are clearly visible (figure 3 in [8] and figure 1(b) in [9]).

- (2) For a disc, the gap width varies non-monotonically with alteration of the collector–cluster distance under a fixed emitter–cluster distance (figure 3 in [9]).

The aim of this work is the computation of the current–voltage characteristic of the molecular transistor based on metal clusters. For this purpose, we use some results from the physics of charged metal clusters [10].

The structure of a granule (or cluster) changes as more and more atoms condense together. A fundamental characteristic of metal clusters, that researchers must explain, is why certain sizes occur preferentially. The elements of the periodic table have heightened stability because those atoms possess a special number of electrons (magic numbers). The tendency for clusters to form in exactly magic sizes arises from the rules of quantum mechanics, which dictate that bound electrons can have only certain energies. So the existence of magic numbers for metal clusters makes sense: they correspond to the number of valence electrons which completely fill one or more shells in a cluster and make it especially stable, by analogy with filled proton and neutron energy shells in atomic nuclei [11]. The calculated magic numbers depend from the shape of cluster (i.e. on the configuration of the ions).

2. Preliminary analysis and formulation of the problem

We consider spherical gold clusters whose radii vary in the range $2R \simeq \{14, 28\} \text{ \AA}$, $R = N_0^{1/3} r_0 \Rightarrow N_0 \simeq \{100, 600\}$, where N_0 is the number of atoms and r_0 is the atom density parameter ($r_0 = 3.01 a_0$ for gold, a_0 is the Bohr radius). Similarly for discs of monatomic thickness: $2R \simeq \{10, 85\} \text{ \AA} \Rightarrow N_0 \simeq \{14, 10^3\}$. We introduce the characteristic Coulomb energy $\tilde{E}_C = e^2/C$, where C is a cluster capacitance [10]. For spheres and discs (as oblate spheroids) we obtain $\tilde{E}_C \simeq \{1.82, 1.06\}$ and $\{3.2, 0.42\}$ eV, respectively. The temperature of the structures is $T \simeq 30$ K.

Let us determine the electron spectrum in spherical and cylindrical wells (see appendix A). For the above mentioned

sizes, the calculation in both cases gives the close values of the spectrum discreteness, $\Delta\epsilon_p \approx \{1.2, 0.3\}$ eV, near to the highest occupied level ϵ^{HO} at $T = 0$. Thus, for the whole range of R in experiments [5–8] we have to deal with a set of open 0D systems (quantum dots). The resulting inequality,

$$\tilde{E}_C \approx \Delta\epsilon_p \gg k_B T, \quad (1)$$

corresponds, apparently, to two coexisting structures in I – V curves: the effects of spectrum quantization and the Coulomb blockade. However, detailed measurements [2, 5–7, 12] performed to date have not yielded an unequivocal conclusion about the effect of electron quantization levels upon the $I(V)$. In our opinion, the discreteness of the spectrum actually determines the zero conductance gap of the I – V curves observed in [5–9].

2.1. Structure in the absence of bias voltage

The left and right electrodes (emitter and collector) represent the electron reservoirs. Each reservoir is taken to be in thermal equilibrium. A continuum of states is assumed in reservoirs, occupied according to the Fermi–Dirac distribution

$$f(\epsilon^{e,c} - \mu_0^{e,c}) = \{1 + \exp[(\epsilon^{e,c} - \mu_0^{e,c})/k_B T]\}^{-1}, \quad (2)$$

where $\mu_0 < 0$ is the electron chemical potential for a semi-infinite metal, $-\mu_0 = W_0$ and W_0 is the electron work function ($W_0 = 5.13$ eV for Au). In all cases the energy $U_0 < \epsilon < 0$ is counted off from the vacuum level and $U_0 < 0$ is the position of the conductivity band of a semi-infinite metal [10].

The electron chemical potential μ^g of a granule in a quantum case can be defined by the normalization condition

$$\sum_{p=1}^{\infty} f(\epsilon_p - \mu^g) \equiv \sum_{p=1}^{\infty} \{1 + \exp[(\epsilon_p - \mu^g)/k_B T]\}^{-1} = N_0, \quad (3)$$

where the sum runs over all one-electron states, N_0 is the total number of thermalized electrons in a cluster and $\mu^g \equiv \mu^g(R)$. If the electron spectrum is known, from equation (3) it is possible to calculate μ^g of cluster Au _{N_0} (gold is univalent).

Figure 2 depicts the chemical potential of some spherical clusters as a function of temperature. Predictably, the

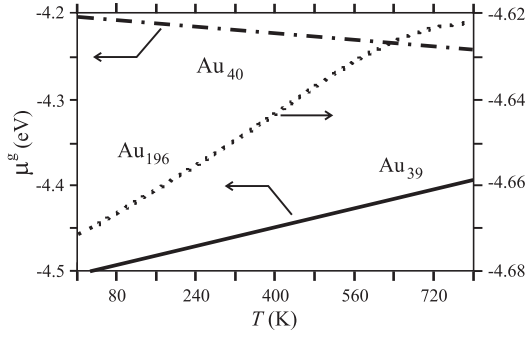


Figure 2. Temperature dependence of chemical potentials of the neutral spherical gold non-magic (Au_{39}) and magic (Au_{40} , Au_{196}) clusters.

dependence is slack and is completely determined by the level hierarchy in dots, and also by the number of electrons. The Fermi level of non-magic clusters coincides with a real level in a cluster. For the magic ones it lies between the energy terms. Calculations show that the temperature gradient of the chemical potential can be both positive and negative, and at some temperatures it can change sign. Similar behaviour $\mu(N_0, T)$ for magic clusters Na_{N_0} has been reported in [13].

A contact potential difference appearing between a cluster and electrodes is

$$\delta\phi = (\mu^g - \mu_0^{e,c})/e. \quad (4)$$

An equilibrium is reached by the charging of a cluster since its capacitance is finite. If $|\mu^g| < |\mu_0^{e,c}|$, a cluster is charged positively by a charge $Q_{\text{eff}}^0 = -e(N' - N_0) > 0$, where N' is determined by the solution of equation (3) replacing $\mu^g \rightarrow -W_0$ for the same spectrum $\{\varepsilon_p\}$ shifted on $-e\delta\phi$, according to Koopmans' theorem [10]. Thus, in the thermodynamic limit we have

$$Q_{\text{eff}}^0 = C\delta\phi. \quad (5)$$

The existence of Q_{eff}^0 has to do with the transparency of the tunnel barriers before application of the voltage. A quasi-classical approximation [14, 15] gives for a metallic sphere of radius R : $\mu^g - \mu_0 = \mu_1/R$, $\mu_1 = 1.9 \text{ eV} \times a_0$, $Q_{\text{eff}}^0 = +0.07e$. In the quantum case, filling levels by electrons we find a highest occupied state, $\varepsilon^{\text{HO}} < 0$, and a lowest unoccupied state, $\varepsilon^{\text{LU}} < 0$, counted off from the vacuum level (figure 1). Then it is necessary to make a replacement $\mu^g \rightarrow \varepsilon^{\text{HO}}$.

Otherwise, in the case $|\mu^g| > |\mu_0|$ (e.g. $\text{Pb}/\text{Au}_{N_0}/\text{Pb}$) the cluster is charged negatively and it is necessary to make a replacement $\mu^g \rightarrow \varepsilon^{\text{LU}}$. The residual effective charge is equal to the non-integer elementary charge e , which is analogous to the charge of a cluster in the 'chemisorption regime'.

The possibility of a fractional charge at tunnelling structures was discussed in [1, 16]. Perhaps this problem is related to fractional quantization (or fractional statistics), when the decoupling of the spin and the electron quantum numbers of a charge is important. In the percolation systems it is supposed that the charge at each granule has a soliton origin. The value of this charge was calculated numerically in [17].

We consider a central electrode–granule in an external electric field. a positive voltage V is applied between the emitter ($V = 0$) and the collector. In the weak electric field

approach we assume that the ionic subsystem of a granule is not deformed, and only the electronic 'cloud', generated by the granule's own valence electrons is deformed.

2.2. Granule under voltage V

The total energy of a granule is a functional of the non-homogeneous electron concentration, $\tilde{E}[n(\mathbf{r})]$. The functional contains a contribution responsible for the interaction of electrons and ions with an external field,

$$e \int [n(\mathbf{r}) - n_i(r)] (\mathbf{E} \cdot \mathbf{r}) d^3r. \quad (6)$$

For simplicity, we suppose that the charge distribution $n_i(r)$ of the ionic subsystem is spherically symmetric.

Let us write down the electron distribution of a granule as

$$n(\mathbf{r}) = n_0(r) + \delta n_1(r) + \delta n_2(\mathbf{r}). \quad (7)$$

Here, $n_0(r)$ is the electron density of a neutral cluster in the absence of an external field,

$$\int n_0(r) d^3r = N_0,$$

δn_1 is the perturbation arising from the charging of the granule,

$$\int \delta n_1(r) d^3r = \Delta N, \quad (8)$$

where $\Delta N > 0$ and $\Delta N < 0$ correspond to negatively and positively charged granules, respectively ($|\Delta N| \ll N_0$). $\delta n_2(\mathbf{r})$ is the next perturbation arising from the external field which is responsible for the polarization of a neutral granule,

$$\int \delta n_2(\mathbf{r}) d^3r = 0. \quad (9)$$

We assume that functions $n_0(r)$ and $n_1(r)$ are spherically symmetrical, and $n_2(\mathbf{r})$ is axially symmetrical. Then one can expand the $\tilde{E}[n(\mathbf{r})]$ in the functional Taylor series down to the second order of smallness with respect to δn_1 and δn_2 ,

$$\begin{aligned} \tilde{E}[n(\mathbf{r})] = & \tilde{E}[n_0(\mathbf{r})] + \sum_j \int \frac{\delta \tilde{E}}{\delta n_j(\mathbf{r})} \delta n_j(\mathbf{r}) d^3r \\ & + \frac{1}{4} \sum_{j,k} \int \int \frac{\delta^2 \tilde{E}}{\delta n_j(\mathbf{r}) \delta n_k(\mathbf{r}')} \delta n_j(\mathbf{r}) \delta n_k(\mathbf{r}') d^3r d^3r' + \dots \end{aligned} \quad (10)$$

Here the functional derivatives are taken at $n(\mathbf{r}) = n_0(r)$, and indexes j and k run 1 and 2 according to the definition (7). The zeroth-order expression $\tilde{E}[n_0(\mathbf{r})] \equiv \tilde{E}_0$ is the total energy of a cluster before the charging ($\Delta N = 0$) and in the absence of an external field ($\mathbf{E} = 0$). The functional derivative

$$\delta \tilde{E} / \delta n(\mathbf{r}) = \mu^g + e(\mathbf{E} \cdot \mathbf{r}). \quad (11)$$

In the absence of charging and an external field $-\mu^g \rightarrow W_0$ as $R \rightarrow \infty$.

Finally, in the semiclassical approximation (see appendix B), we get

$$\tilde{E} = \tilde{E}_0 + \mu^g \Delta N - e \Delta N \eta V + (\Delta N)^2 \tilde{E}_C / 2 - \alpha \mathbf{E}^2 / 2. \quad (12)$$

The tunnelling of a single electron through barriers is determined by the tunnel rates $\Gamma^{e,c}$, which depend on the junction geometry and the voltage fraction ηV . In general, their evaluation is a far from trivial problem [2, 16]. We assume that $\Gamma^{e,c}$ are small and the temperature is not too low, i.e. $k_B T > \hbar(\Gamma^e + \Gamma^c) \ll \min\{\Delta\varepsilon_p, \tilde{E}_C\}$.

By analogy with the theory of [18], we introduce the partial tunnelling rates from electrodes to a granule

$$\vec{\omega}_n^e = 2 \sum_p \Gamma(\vec{\varepsilon}^e) f(\vec{\varepsilon}^e - \mu_V^e) [1 - f(\vec{\varepsilon}^e - \vec{\mu}_C^e)], \quad (20)$$

$$\overleftarrow{\omega}_n^c = 2 \sum_p \Gamma(\overleftarrow{\varepsilon}^c) f(\overleftarrow{\varepsilon}^c - \mu_V^c) [1 - f(\overleftarrow{\varepsilon}^c - \overleftarrow{\mu}_C^c)], \quad (21)$$

and from a granule to the electrodes

$$\overleftarrow{\omega}_n^e = 2 \sum_p \Gamma(\overleftarrow{\varepsilon}^e) [1 - f(\overleftarrow{\varepsilon}^e - \mu_V^e)] f(\overleftarrow{\varepsilon}^e - \overleftarrow{\mu}_C^e), \quad (22)$$

$$\vec{\omega}_n^c = 2 \sum_p \Gamma(\vec{\varepsilon}^c) [1 - f(\vec{\varepsilon}^c - \mu_V^c)] f(\vec{\varepsilon}^c - \vec{\mu}_C^c), \quad (23)$$

where the factor 2 takes into account the spin degeneration of levels in the electrodes. In view of the applied voltage (and charging of a granule) the spectra (see equations (17)–(19)) and the chemical potentials are shifted in the distributions (2) and (3):

$$\begin{aligned} -\mu_V^e &\equiv W_0^e, & \overleftarrow{\mu}_C^e &= \mu^g - e\delta\phi + \tilde{E}_C(n \mp 1/2) - e\eta^+ V, \\ \overleftarrow{\mu}_C^c &= \mu - e\delta\phi + \tilde{E}_C(n \pm 1/2) + e(1 - \eta^+) V, \\ \mu_V^c &= \mu_0^c - eV. \end{aligned}$$

As a first approximation of the perturbation theory [10], for small V , μ^g is determined not only by the formal shift of the well depth but also by the number of conduction electrons in the granule ($N = N_0 + n_q$, $n_q = n + [Q_{\text{eff}}^0]/e$). The use of chemical potentials is correct in a quasi-equilibrium state, i.e. when the intervals between acts of tunnelling are much longer than the relaxation time. It is also supposed that the external electric field and the Coulomb blockade do not disrupt the degeneration of levels.

Let us denote the total electron transition rates from/to leads into/out the cluster, as

$$\omega_n^{\text{in}} = \vec{\omega}_n^e + \overleftarrow{\omega}_n^c, \quad \omega_n^{\text{out}} = \overleftarrow{\omega}_n^e + \vec{\omega}_n^c.$$

In the limit of weak tunnelling, the probability P_n of the finding of n above mentioned electrons at the central electrode is defined by the master equation in the stationary limit

$$\dot{P}_n = \omega_{n+1}^{\text{out}} P_{n+1} + \omega_{n-1}^{\text{in}} P_{n-1} - (\omega_n^{\text{in}} + \omega_n^{\text{out}}) P_n = 0. \quad (24)$$

The requirement of stationarity gives the recurrent relation

$$P_{n+1} = P_n \omega_n^{\text{in}} / \omega_{n+1}^{\text{out}}. \quad (25)$$

The dc current flowing through a metallic quantum dot (with restriction on its instability (14)), is determined as

$$I = -e \sum_{n_{\text{min}} < 0}^{n_{\text{max}} > 0} P_n (\vec{\omega}_n^e - \overleftarrow{\omega}_n^c) = -e \sum_{n_{\text{min}} < 0}^{n_{\text{max}} > 0} P_n (\overleftarrow{\omega}_n^e - \vec{\omega}_n^c). \quad (26)$$

Let us consider the case of ‘strong quantization’ for the electron spectrum:

$$\Delta\varepsilon_p \gg \tilde{E}_C.$$

This regime is hypothetically reached by a significant increase in the cluster capacitance (the cluster shape must be changed to a needle-like or disc-like one under the condition that its volume is fixed (see, e.g., [10]). Thus the charge Q_{eff}^0 in (5), which provides a contact potential difference, is proportional to the capacitance and can have a large magnitude. When the voltage is applied, the charge, which is caused by the transferring surplus electrons, is much less than Q_{eff}^0 . Therefore it has an insignificant influence on the cluster energetics. In reality, the inequality $\Delta\varepsilon_p \gg \tilde{E}_C$ is not possible even for a long atomic chain [10]. Nevertheless, this case is useful from the methodical point of view for analysing the current gap in the I – V characteristics.

As an assumption, we use fixed tunnel rates at the Fermi level in the emitter. This is correct for small voltages, $eV \ll W_0$. Neglecting in (17)–(19) terms $\sim \tilde{E}_C$, it is easy to obtain the result, similar to [18]:

$$I = I_0 \sum_p [f(\varepsilon^e - \mu_0^e) - f(\varepsilon^e - \mu_V^e)], \quad (27)$$

where $I_0 = 2e\Gamma^e\Gamma^c/(\Gamma^e + \Gamma^c)$.

The expressions in this section are written down for $V > 0$. In the case $V < 0$, the $I(V)$ can be easily obtained if we set $V = 0$ on a collector and $V > 0$ on the emitter, and use $\eta^- = 1 - \eta^+$.

In the general case, for calculation of I – V (26) it is necessary to know probabilities P_n . Their statistical determination is a complicated problem [24]. In the experiments, the size of the cluster and its location are known only approximately, therefore detailed calculations of P_n are not suitable. Using the recurrent relations we can find the ratios $P_{n \neq 0}/P_0$.

4. Application and discussion

In accordance with our previous results [14], $|\mu^g| < |\mu_0|$, therefore the cluster is charged positively before application of the voltage. The size dependence of a charge $Q_{\text{eff}}^0(N_0)$ for the gold clusters is demonstrated in figure 3. For the above mentioned sizes of spherical clusters, $Q_{\text{eff}}^0 < e$. However, Q_{eff}^0 can accept values larger than e for discs of monatomic thickness. Additional charging of the cluster can lead to Coulomb instability, because the quantity Q_{eff}^0 is close to a critical charge [10]. Moreover, cluster’s anomalous electrostriction is possible as a result of the charging [25].

Setting the collector–granule distance d_c , parameter $\beta = \Gamma^e/\Gamma^c$ and using the recurrent relation (25) for equation (26), it is possible to calculate the reduced dc current $\tilde{I} \equiv I/(eP_0\Gamma^e)$. We do not evaluate the threshold voltages separately, in our scheme they appear automatically.

The results of calculations of the I – V characteristics for the structures Au/Au $_{N_0}$ /Au, based on spherical clusters, are presented in figure 4. For completeness of analysis, the voltage behaviour of the reduced probabilities $\tilde{P}_n(V) \equiv P_n/P_0$ and the difference of electron streams $\Delta\omega_n = \overleftarrow{\omega}_n^e - \vec{\omega}_n^c$ are also given.

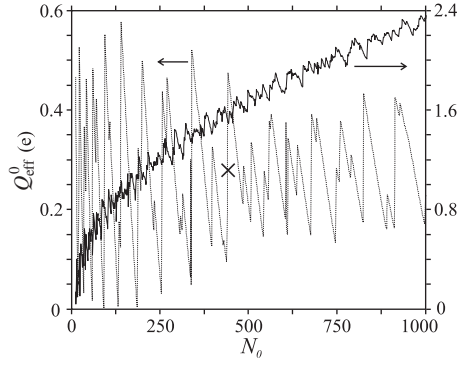


Figure 3. The calculated size dependence of the residual effective charge Q_{eff}^0 (5) for the structure Au/Au $_{N_0}$ /Au based on clusters of various shapes: sphere (dotted line) and disc (solid line). For illustration, Q_{eff}^0 of a magic sphere Au $_{439}$ is marked as \times .

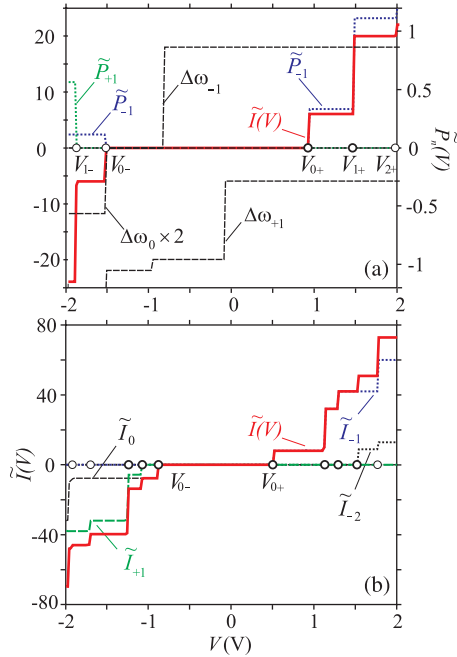


Figure 4. The current–voltage curves (solid lines) and their components, calculated from equation (26) ($\beta = 1$, $\eta^+ = 0.1$, $T = 30$ K). $\Delta\omega_n$ is given in Γ^c units: (a) Au/Au $_{40}$ /Au; (b) Au/Au $_{100}$ /Au;

The current jumps are stipulated by the jumps of $\tilde{P}_n(V)$ and $\Delta\omega_n(V)$, because the current is formed by their product. As one can surmise, the jump of probability $\tilde{P}_{-1}(V)$ causes the current jump in the threshold voltage V_{0+} .

Making use of the equality $\tilde{I} \equiv \sum_n \tilde{I}_n(V)$ in accordance with equation (26) one can also fix the ‘threshold’ values of n . As is seen from figure 4(b), the role of partial current components \tilde{I}_n (with $|n| > 1$) grow with increasing N_0 . The charging leads to an energy shift of spectrum according to equations (17)–(19). Thus the different parts of a spectrum are involved during tunnelling.

The current gap width, $\Delta V_g = V_{0+} + |V_{0-}|$, for all structures is determined by values $n = 0, -1$. The probability P_{-1} prevails over P_{+1} , because the ‘granule–collector’ electron

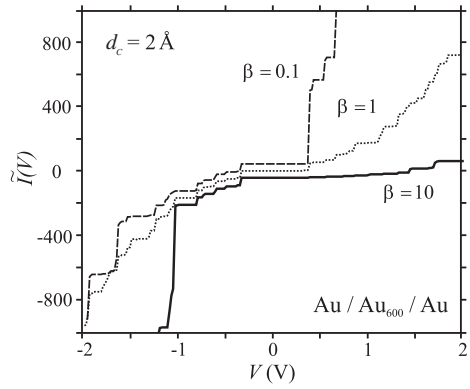


Figure 5. Calculated I – V curves at $T = 30$ K for a structure based on spherical clusters. For presentation the curves are shifted slightly vertically.

stream is more than a ‘emitter–granule’ one and the granule is charged positively (i.e. $n < 0$). The conductance gap boundaries can be defined by the charging energy and the position of the lowest unoccupied level as

$$|V_{0\pm}| = \frac{\tilde{E}_C/2 + \Delta\varepsilon}{(2 - \eta^\pm)},$$

where $\Delta\varepsilon = \{\mu^g - \varepsilon^{\text{LU}} \text{ and } 0\}$ for the magic and non-magic clusters, respectively. For large granules $\Delta V_g \rightarrow 0$ as $R \rightarrow \infty$.

Within the applied voltage the I – V characteristics versus η^+ are shifted to the right and the gap width decreases a little. The calculated I – V curves of the structure Au/Au $_{600}$ /Au for fixed η^+ ($d_c = 2$ Å) and different β are shown in figure 5. The current gap is practically independent of β ; however, the current jumps are strongly dependent on the value of β , which, in its turn, has no influence on threshold voltages.

In order to illustrate our results, in figure 6 we compare the size dependences $\Delta V_g(N_0)$ calculated from equations (26) and (27) for spheres and discs. The largest quantities ΔV_g correspond to the magic granules, for which $\Delta\varepsilon \neq 0$. For the case of ‘strong quantization’ the size of the current gap for non-magic clusters is equal to zero explicitly, because the emitter Fermi level is in line with the closed levels in the cluster. Calculations demonstrate the non-monotonic dependence $\Delta V_g(N_0)$. These results also show that charging leads to the growth of a gap.

The actual forms of dependence $\Delta V_g(d_c)$ for the structure based on a magic disc Au $_{178}$ ($R \approx 35$ Å) are plotted in figure 7. In experiments [8, 9] the gap varied as $0.8 \rightarrow 0.4 \rightarrow 0.7$ V for the cyclic variation of $d_c \approx 1 \rightarrow 2 \rightarrow 1$ Å. The reasons for such numerical distinction of our results are apparently due to neglecting the role of nonlinearities in the strong electric field and in the energy dependence of tunnelling rates. At high rates the capacitance ceases to be classical and can grow strongly ($\tilde{E}_C \rightarrow 0$) [26, 27], showing a non-monotonic dependence from Γ^c . This means that, in reality, we deal with the intermediate cases (between limiting estimations from equations (26) and (27) in figure 7).

Let us discuss other features of the tunnel structure. In spite of the fact that the emitter and a collector are made of one material, the chemical potentials of electrons are not equal

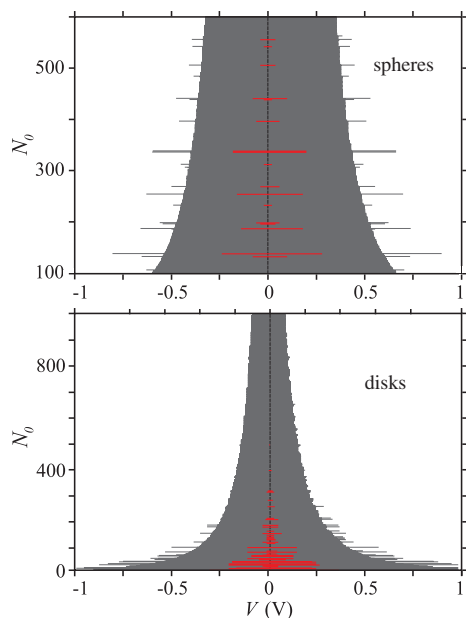


Figure 6. The current gap calculated from equation (26) ($d_c = 2 \text{ \AA}$ and $\beta = 10$). Solid (red) lines show the gaps calculated from equation (27) for the case of ‘strong quantization’.

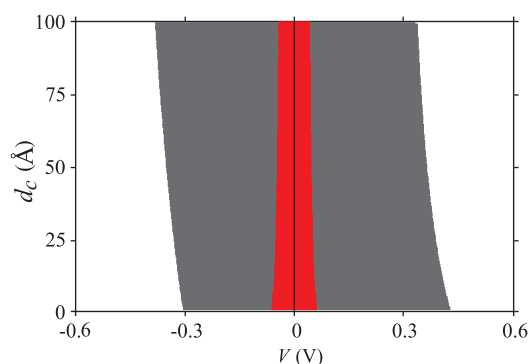


Figure 7. Calculated current gaps ($\beta = 10$) from equations (26) and (27) for the magic disc Au_{178} .

to each other: the emitter is represented by a thick film of Au (111), and a collector by a polycrystal of Au. Their work functions are different [28]. Also, the emitter is covered with a dielectric film that influences the electron work function. We can estimate this contribution.

Proceeding from indirect measurements [29], the work function decreases with growth of the dielectric constant ϵ of the coating. The calculations of the electron work function W_d for cylindrical nanowires in a dielectric confinement are done in [30]: W_d decreases by approximately 20% in magnitude as ϵ rises from 1 to 4. The basic contribution can thus be related to a change in the contribution of the electrostatic dipole barrier to the work function of the gold–vacuum system, which can be up to 30% [28]. Hence, this contribution also puts an upper limit on the change of W_d for a metal–dielectric–vacuum system. Owing to $W_d < W_0$ the inequality $|\mu^g| > W_d$ is possible, which can lead to negative charging of the cluster before the application of the voltage. Finally, the metal–nonmetal transition for the gold cluster can appear [31].

It is necessary to notice that the existence of disc-shaped Au nanoclusters with monolayer thickness, considered to be grown on the alkanethiol monolayer, was first reported in [8, 9], and has not been reproduced by other researchers. We hope that future experimental investigations will confirm their results. Nevertheless, our theoretical modelling can be applied to such physically reliable systems as structures based on the spherical gold clusters [5–7] and cylindrical CdSe finite nanowires [32], etc.

5. Summary

In the framework of the particle-in-a-box model for spherical and disc-shaped gold clusters, the electron spectrum was calculated. In this model, the work function of clusters is smaller than that of semi-infinite gold electrodes. This results in the appearance of a contact potential difference between a cluster and electrodes. The residual effective charge is equal to a non-integer elementary charge e , which is analogous to the charge of a cluster in the ‘chemisorption regime’. For small spherical clusters, the positive charge is less than e . However, this charge can have a value larger than e for discs of monoatomic thickness. Additional charging of the clusters can lead to Coulomb instability because it is close to the critical charge. Charging results in an energy shift of the spectrum.

The current–voltage characteristics were analysed taking into account the contact potential difference. For single-electron molecular transistors based on small gold clusters the current gap and its voltage asymmetry were computed. The largest gaps correspond to the magic granules. For the case of ‘strong quantization’, the size of a current gap for non-magic clusters is equal to zero explicitly, because the emitter Fermi level is in line with the closed levels in cluster. We derive a simple expression for the size dependence of the current gap width, which takes into account the Coulomb blockade and discreteness of the energy levels. The results show that charging leads to the growth of a gap.

Acknowledgments

We are grateful to W V Pogoso for reading the manuscript. This work was supported by the Ministry of Education and Science of Ukraine (Programme ‘Nanostructures’) and the Samsung Corporation.

Appendix A. Electron spectrum in cylindrical-like clusters

As an approximation, the profile of the one-electron effective potential in the cluster can be represented as a potential well of depth $U_0 < 0$. The three-dimensional Schrödinger equation for a quantum box can be separated into one-dimensional equations. The spectra of wave numbers in spherical and cylindrical potential wells are determined from the continuity condition of a logarithmic derivative of the wavefunction on the boundaries. For a disc of radius R and thickness H it is necessary to solve the equation:

$$k_{nm} \frac{I'_m(k_{nm}R)}{I_m(k_{nm}R)} = \chi_{nm} \frac{K'_m(\chi_{nm}R)}{K_m(\chi_{nm}R)}. \quad (\text{A.1})$$

Here I_m is the Bessel function, K_m is the McDonald function, the stroke denotes a derivative over an argument, $k_{nm} = \sqrt{k_0^2 - \alpha_{nm}^2}$, $\hbar k_0 = \sqrt{2m_e|U_0|}$, and m_e is the electron mass. The $n = 1, 2, 3 \dots$ number the roots of the equation (A.1) for fixed $m = 0, \pm 1, \pm 2 \dots$

Using the perturbation theory [10], the finite well problem can be reduced to the infinite well one:

$$k_{nm} = k_{nm}^{(0)} + k_{nm}^{(1)} + \dots, \quad |k_{nm}^{(1)}/k_{nm}^{(0)}| \ll 1,$$

where $k_{nm}^{(0)}$ defines the spectrum of the infinitely deep well. Numbers $k_{nm}^{(0)}$ are determined by solutions of the equation

$$I_m(k_{nm}^{(0)}R) = 0.$$

In the first approximation we have

$$k_{nm}^{(1)} = \frac{k_{nm}^{(0)}K_m(\alpha_{nm}^{(0)}R)}{R\alpha_{nm}^{(0)}K'_m(\alpha_{nm}^{(0)}R)}.$$

The estimation gives $k_{nm}^{(1)} < 0.07k_{nm}^{(0)}$, confirming sufficient accuracy of the theory.

Quantization of the wavevector k_s along the cylinder axis is determined by the solution of the equation:

$$k_s H = s\pi - 2 \arcsin(k_s/k_0),$$

where s is the integer number. Neglecting the area near the cylinder edges, the energy spectrum is calculated in a simple way as follows:

$$\varepsilon_{nms} = U_0 + \frac{\hbar^2}{2m_e}(k_{nm}^2 + k_s^2).$$

In addition to the spin degeneration, there is a double degeneration with respect to the sign of index m , since $k_{n,m} = k_{n,-m}$. Further, the spectrum of the cluster is denoted as ε_p , $p = 1, 2, 3 \dots$ is the number of *one-electron state*. All levels are numbered in order of increasing energy.

Appendix B. Energy of a cluster in an external electrical field

Using spherical coordinates, we remove the centre point $z = 0$ from an emitter in the centre of a granule, and we direct a z -axis from a collector to the emitter under the conservation of the potential difference between them. Then an electric field $\mathbf{E} = |\mathbf{E}|\hat{\mathbf{z}}$, where $\hat{\mathbf{z}}$ is a unit vector along a z -axis.

As the surplus charge is effectively distributed over a surface, it is quite reasonable for estimation to use the form

$$\delta n_1(r) = \begin{cases} 0, & 0 < r < R - b, \\ \tilde{n}, & R - b < r < R, \\ 0, & R > 0. \end{cases} \quad (\text{B.1})$$

Using condition (8), we obtain the following expression for surface concentration:

$$\tilde{n} = \frac{\Delta N}{\Omega(3\xi - 3\xi^2 + \xi^3)},$$

where $\Omega = 4\pi R^3/3$, and $\xi = b/R$ is the small parameter.

Then, we use the linear response approach (see, e.g., [19])

$$\delta n_2(r, \theta) = Y(r) |\mathbf{E}| \cos \theta. \quad (\text{B.2})$$

The spherically symmetric function $Y(r)$ in (B.2) is determined from the normalization condition (9) and a global minimum of the functional, $\delta \tilde{E}[n(\mathbf{r})] \rightarrow 0$.

One of the terms of interest to us is

$$-e \int \delta n_1(r) \varphi(z) d^3 r,$$

where φ is an external electrostatic potential. In the case of $V > 0$ and vacuum collector-emitter space $\varphi(z) = V(z - d_c - L/2)/d$, where $d = d_c + L + d_e$. After the integration in spherical coordinates, the term, which is proportional to z , vanishes, and, as a result, we have $-e\Delta N\eta V$; η is a fraction of a voltage.

The other three terms

$$\int \frac{\delta n_1(\mathbf{r})\delta n_2(\mathbf{r}') + \delta n_1(\mathbf{r})\delta n_1(\mathbf{r}') + \delta n_2(\mathbf{r})\delta n_2(\mathbf{r}')}{|\mathbf{r} - \mathbf{r}'|} d^3 r d^3 r' \quad (\text{B.3})$$

give a basic contribution to the second order of expansion (10). The first integral in equation (B.3) for the functions (B.1) and (B.2) vanishes after the integration on corners and the second one equals

$$(\Delta N)^2 \frac{\tilde{E}_C}{2} \left(1 + \frac{\xi}{3}\right).$$

The third integral was calculated earlier for the definition of the polarizability of a cluster $\alpha = -(4\pi/3) \int_0^\infty Y(r)r^3 dr \equiv R_{\text{eff}}^3 \approx R^3$ [19]. Finally we obtain equation (12).

References

- [1] Likharev K K 1999 *Proc. IEEE* **87** 606
- [2] von Delft J and Ralph D C 2001 *Phys. Rep.* **345** 61
- [3] Aleiner I L, Brouwer P W and Glazman L I 2002 *Phys. Rep.* **358** 309
- [4] Semrau S, Schoeller H and Wenzel W 2005 *Phys. Rev. B* **72** 205443
- [5] Ohgi T, Sheng H-Y, Dong Z-C, Nejh H and Fujita D 2001 *Appl. Phys. Lett.* **79** 2453
- [6] Ohgi T and Fujita D 2002 *Phys. Rev. B* **66** 115410
- [7] Ohgi T and Fujita D 2003 *Physica E* **18** 349
- [8] Ohgi T, Sakotsubo Y, Ootuka Y and Fujita D 2004 *Appl. Phys. Lett.* **84** 604
- [9] Wang B, Xiao X, Huang X, Sheng P and Hou J G 2000 *Appl. Phys. Lett.* **77** 1179
- [10] Hou J G, Wang B, Yang J, Wang X R, Wang H Q, Zhu Q and Xiao X 2001 *Phys. Rev. Lett.* **86** 5321
- [11] Pogosov V V, Kurbatsky V P and Vasyutin E V 2005 *Phys. Rev. B* **71** 195410
- [12] Brack M 1993 *Rev. Mod. Phys.* **65** 677
- [13] Brack M 1997 *Sci. Am.* **277** 30
- [14] Gubin S P, Gulayev Yu V, Khomutov G B, Kislov V V, Kolesov V V, Soldatov E S, Sulaimankulov K S and Trifonov A S 2002 *Nanotechnology* **13** 185
- [15] Kurkina L I and Farberovich O V 1996 *Solid State Commun.* **98** 469
- [16] Pogosov V V 1990 *Solid State Commun.* **75** 469
- [17] Kiejna A and Pogosov V V 1996 *J. Phys.: Condens. Matter* **8** 4245
- [18] Azbel' M Ya 1998 *Phys. Usp.* **41** 543
- [19] Parthasarathy R, Lin X-M, Elteto K, Rosenbaum T and Jaeger H M 2004 *Phys. Rev. Lett.* **92** 076801

- [18] Averin D V, Korotkov A N and Likharev K K 1991 *Phys. Rev. B* **44** 6199
- [19] Snider D R and Sorbello R S 1983 *Phys. Rev. B* **28** 5702
- [20] Wood D M and Ashcroft N W 1982 *Phys. Rev. B* **25** 6255
- [21] Sokolov A V 1967 *Optical Properties of Metals* (New York: Elsevier)
- [22] Kurbatsky V P and Pogosov V V 2000 *Tech. Phys. Lett.* **26** 1020
- [23] Beenakker C W J 1991 *Phys. Rev. B* **44** 1646
- [24] Brack M, Genzken O and Hansen K Z 1991 *Z. Phys. D* **21** 65
- [25] Pogosov V V 1992 *Solid State Commun.* **81** 129
- [26] Wang J, Guo H, Mozos J-L, Wan C C, Taraschi G and Zheng Q 1998 *Phys. Rev. Lett.* **80** 4277
- [27] König J and Schoeller H 1998 *Phys. Rev. Lett.* **81** 3511
- [28] Pogosov V V and Shtepa O M 2002 *Ukr. Phys. J.* **47** 1065 (Preprint [cond-mat/0310176](#))
- [29] Modinos A 1984 *Field, Thermionic and Secondary Electron Emission Spectroscopy* (London: Plenum)
- [30] Smogunov A N, Kurkina L I, Kurganskii S I and Farberovich O V 1997 *Surf. Sci.* **391** 245
- [31] Boyen H-G, Ethirajan A, Kastle G, Weigl F, Ziemann P, Schmid G, Garnier M G, Buttner M and Oelhafen P 2005 *Phys. Rev. Lett.* **94** 016804
- [32] Millo O, Katz D, Steiner D, Rothenberg E, Mokari T, Kazes M and Banin U 2004 *Nanotechnology* **15** R1